

Instantaneous Spectra Analysis of Pulse Series - Application to Lung Sounds with Abnormalities

Fumihiko Ishiyama
NTT Inc., Tokyo, Japan
fumihiko.ishiyama@ntt.com

Abstract

The origin of the “theoretical limit of time-frequency resolution of Fourier analysis” is from its numerical implementation, especially from an assumption of “Periodic Boundary Condition (PBC),” which was introduced a century ago. We previously proposed to replace this condition with “Linear eXtrapolation Condition (LXC),” which does not require periodicity. This feature makes instantaneous spectra analysis of pulse series available, which replaces the short time Fourier transform (STFT). We applied the instantaneous spectra analysis to two lung sounds with abnormalities (crackles and wheezing) and to a normal lung sound, as a demonstration. Among them, crackles contains a random pulse series. The spectrum of each pulse is available, and the spectrogram of pulse series is available with assembling each spectrum. As a result, the time-frequency structure of given pulse series is visualized.

1 Introduction

The origin of the “theoretical limit of time-frequency resolution of Fourier analysis” was thought to be definite, but it was found that it is from its numerical implementation, and therefore it is not “theoretical” [1, 2]. The point is that the “Periodic Boundary Condition (PBC),” shown in Fig. 1(a), which is implicitly introduced to the conventional numerical process of Fourier calculation, and which implicitly assumes that “the time series for analysis is infinitely periodic.” This assumption was required to fulfill the infinite integral for Fourier analysis

$$S(f) = \int_{-\infty}^{\infty} s(t)e^{-2\pi ift} dt. \quad (1)$$

In regard to this matter, we previously showed that there is another way [1] to fulfill the infinite integral, and the way “Linear eXtrapolation Condition (LXC)” shown in Fig. 1(b) goes beyond the limitation. It is because the LXC does not require periodicity, and this feature makes instantaneous spectra analysis of pulse series available.

Therefore, we propose to replace the conventional PBC-Fourier analysis with the LXC-Fourier analysis. As is shown below, the proposed LXC-Fourier analysis theoretically includes the conventional PBC-Fourier analysis.

The origin of the PBC will be on the dawn of the quantum mechanics around 1930s, that condition is commonly used such as in the field of solid state physics.

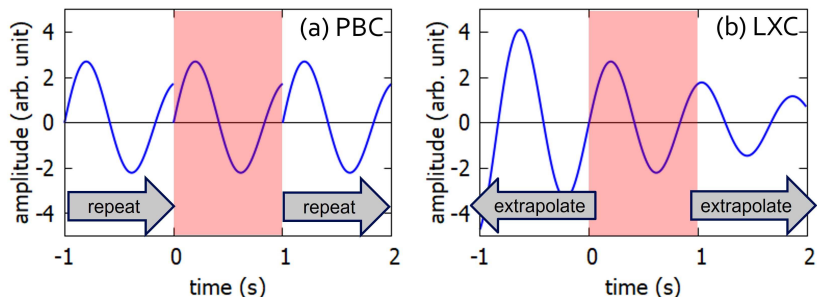


Figure 1: Waveform inside hatched area is given time series for analysis. (a) Conventional Periodic Boundary Condition (PBC), which repeats given waveform infinitely [3], and (b) proposed Linear eXtrapolation Condition (LXC), which linearly extrapolates given waveform [1].

In that historical background, one of the first applications of the PBC on numerical analysis is the work by Walker (1931) [3], which is the ascending of various numerical methods [2] such as the auto correlation, linear prediction, and maximum entropy method.

We apply the LXC-Fourier analysis to the instantaneous spectra analysis of lung sounds with abnormalities such as “crackles” and “wheezing” [4], which are recorded using a digital stethoscope, as a demonstration. Among them, “crackles” contains a random pulse series.

As the conventional PBC-Fourier analysis requires infinite periodicity, it is not suitable for this random pulse series. In contrast, proposed LXC-Fourier analysis, which linearly extrapolates each pulse, is available.

The spectrum of each pulse is available, and the spectrogram of pulse series is available with assembling each spectrum. As a result, the time-frequency structure of given pulse series is visualized.

In the following sections, we introduce the method of LXC-Fourier analysis, show what are available with the method, apply the method to the instantaneous spectra analysis of various lung sounds, one of which contains a random pulse series, and conclude this paper.

2 LXC-Fourier analysis

The LXC-Fourier analysis [1, 2, 5, 6] is understood as an expansion of the concept of “instantaneous frequency” by van del Pol [7]. The concept corresponds to the flame work of frequency modulation (FM), and we add the concept of amplitude modulation (AM) in it. Then, we have a series expansion with AM-FM oscillations, which is shown below.

Remind that the conventional PBC-Fourier analysis is a series expansion without FM, and also without AM. Therefore, another flame work for the LXC-Fourier analysis is required.

In addition, we introduce the concept of “local linearization” by Kubo [8], and we numerically calculate local linearized solution. This concept is required to obtain a unique series expansion [9, 10, 11].

2.1 Model equation

We expand the given time series $S(t) \in \mathbb{R}$ with general complex functions $H_m(t) \in \mathbb{C}$ as

$$S(t) = \sum_{m=1}^M e^{H_m(t)}, \quad (2)$$

where M is the number of complex functions.

The complex functions are expressed as

$$H_m(t) = \ln c_m(t_0) + \int_{t_0}^t [2\pi i f_m(\tau) + \lambda_m(\tau)] d\tau, \quad (3)$$

where $f_m(t) \in \mathbb{R}$ represents the FM terms, which is known as instantaneous frequency [7] by van der Pol, $\lambda_m(t) \in \mathbb{R}$ represents the AM terms, which is our original [5, 6], and $c_m(t_0) \in \mathbb{C}$ represents the amplitudes of the terms at $t = t_0$.

This expansion corresponds to a mode decomposition with general complex functions, noting that

$$H'_m(t) = 2\pi i f_m(t) + \lambda_m(t). \quad (4)$$

Additionally, note that the case

$$H'_m(t) = 2\pi i \frac{m}{M\Delta T}, \quad (5)$$

becomes conventional PBC-Fourier series expansion

$$S(t) = \sum_{m=1}^M e^{H_m(t)} = \sum_{m=1}^M c_m(t_0) e^{2\pi i \frac{m}{M\Delta T}(t-t_0)}, \quad (6)$$

itself. That is, our model equation contains PBC-Fourier analysis as a special case, and is a natural expansion.

2.2 Locally linearized solution

It is known that this kind of AM-FM series expansion does not have a unique solution [9, 10, 11]. Daubeshies presented such an example [9] with a simple time series

$$S(t) = \frac{1}{4} \cos(\Omega - \gamma)t + \frac{1}{4} \cos(\Omega + \gamma)t + \frac{5}{2} \cos \Omega t \quad (7)$$

$$= \left(2 + \cos^2 \frac{\gamma}{2} t\right) \cos \Omega t. \quad (8)$$

It means that there are multiple expressions for a single waveform, and each expression has its own spectrogram [11] shown in Fig. 2.

Therefore, we introduce the concept of ‘‘local linearization’’ by Kubo [8] to overcome this issue [10], which corresponding to selecting Eq. (7) and the LXC-Fourier analysis.

For the purpose, we expand Eq. (2) as

$$S(t)|_{t \sim t_k} \simeq \sum_{m=1}^M e^{H_m(t_k) + H'_m(t_k)(t-t_k) + O((t-t_k)^2)}, \quad (9)$$

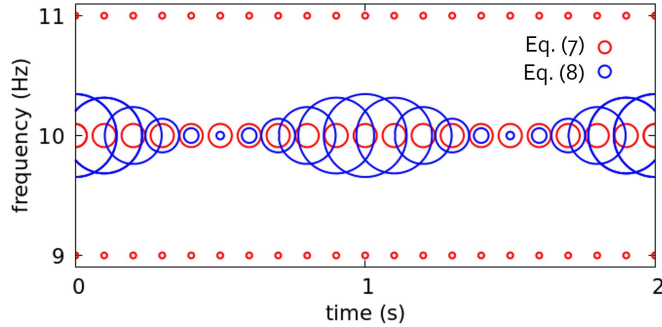


Figure 2: Two spectrograms for single waveform [11].

around $t \sim t_k = t_0 + k\Delta T$, consider a short enough time width, and ignore the higher order terms $O((t - t_k)^2)$.

Then, the equation becomes a simple linear equation

$$S(t)|_{t \sim t_k} \simeq \sum_{m=1}^M e^{H_m(t_k) + H'_m(t_k)(t-t_k)} \quad (10)$$

$$= \sum_{m=1}^M c_m(t_k) e^{[2\pi i f_m(t_k) + \lambda_m(t_k)](t-t_k)}, \quad (11)$$

and we can obtain unique $H'_m(t_k)$ easily by applying the numerical method of linear predictive coding (LPC) with N samples, noting that we must use a non-standard numerical method [2, 12] to hold the condition LXC shown in Fig. 1(b). The standard method of LPC is not adequate, because it contains the unfavorable condition PBC by Walker [3] shown in Fig. 1(a), and an unfavorable approximation by Itakura [13] to reduce computation cost.

Subsequently, we calculate the complex amplitudes $c_m(t_k)$ of the terms $c_m(t_k)e^{H'_m(t_k)(t-t_k)}$ as

$$\arg \min_{c_m(t_k)} \sum_{n=0}^{N-1} \left(S(t_k + n\Delta T) - \sum_{m=1}^M c_m(t_k) e^{nH'_m(t_k)\Delta T} \right)^2. \quad (12)$$

2.3 Instantaneous spectrum

The equation for instantaneous spectrum is given as follows: we transform Eq. (11) with a complex integral as

$$\begin{aligned} F(f, t_k) &= \int_C S(t)|_{t \sim t_k} e^{-2\pi i f t} dt \\ &= \sum_m \frac{c_m(t_k)}{\lambda_m(t_k) + 2\pi i (f_m(t_k) - f)}. \end{aligned} \quad (13)$$

As Eq. (13) is for continuous systems, some modifications to adopt for discrete systems are required. That is, specifically, a modification from a Fourier transform to a Fourier series expansion.

For example, when $\lambda_m(t_k) = 0$, Eq. (13) is unbound at $f = f_m(t_k)$, and is not practical. The practical value is the maximum value $|c_m(t_k)|$ for discrete systems.

Therefore, we take the absolute value of each term, and adjust the maximum values at $f = f_m(t_k)$ so as to be $|c_m(t_k)|$ [2].

$$F_{\text{disc}}(f, t_k) = \sum_m \left| \frac{c_m(t_k) \lambda_m(t_k)}{\lambda_m(t_k) + 2\pi i (|f_m(t_k)| - f)} \right| \quad (14)$$

This equation has several merits [2, 5]. For example, the instantaneous spectrum of each term is available, and this feature is valuable for signal separation, as we show below. In addition, $F_{\text{disc}}(f, t_k)^2$ becomes power spectrum, corresponding to the conventional Fourier power spectrum.

Another equation for instantaneous spectrum

$$F_{\pm}(f, t_k) = \sum_m \left| \frac{c_m(t_k)}{\lambda_m(t_k) + 2\pi i (|f_m(t_k)| - f)} \right| \lambda_m(t_k), \quad (15)$$

is also available with our method. Negative intensity becomes available with this equation. The positive intensity means that the signal is growing ($\lambda_m(t_k) > 0$), and the negative intensity means that the signal is decaying ($\lambda_m(t_k) < 0$).

2.4 Revised time-frequency resolution

We briefly demonstrate how LXC-Fourier analysis works [12]. The source code and its execution output of the followings are shown in the reference.

The time series for analysis shown in Fig. 3(a) is

$$S(t) = 0.01 + \sin 2\pi t, \quad (16)$$

and we take twelve samples with a sampling frequency of 10 Hz, as shown in the figure. The samples correspond to 1.2 cycles of the oscillation.

Following this, we apply the LXC-Fourier analysis to the twelve samples, and plot each obtained term in Eq. (14) in Fig. 3(b).

In addition, we plot the PBC-Fourier spectrum from the same twelve samples in the figure, which corresponds to a bin of short time Fourier transform (STFT).

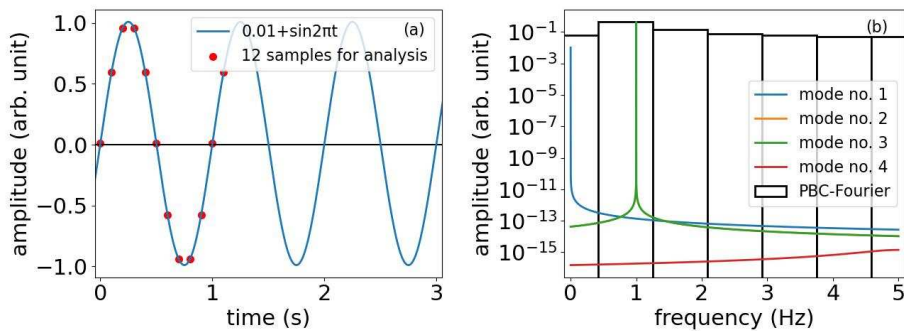


Figure 3: (a) Waveform, and 12 samples for analysis. (b) Obtained spectra with LXC- and PBC-Fourier analysis [12].

Four LXC-Fourier spectra (no. 1 to 4) are shown in Fig. 3(b). Each spectrum corresponds to (no. 1) a constant term with amplitude 0.01, (no. 2 and 3, the same spectra) a sinusoidal time series with a frequency of 1 Hz, and (no. 4) computational error, which corresponds to white noise on the time series.

Note that white noise on the given time series (no. 4) is obtained as a mode with a flat spectrum, and we can remove this unnecessary term from Eq. (14) for plotting spectrum.

Obtained numerical results for no. 1 to 3 are shown in Table 1. We can

term	frequency (Hz)	amplitude
no. 1	0.0	0.00999999999999492205
no. 2 & 3	0.9999999999999438	1.00000000000004858

obtain this numerical resolution with using twelve samples. In contrast, the resolution with PBC-Fourier analysis is restricted to $1/1.2$ Hz.

As another demonstration, a spectrogram of FM time series using LXC-Fourier analysis is shown in Fig. 4.

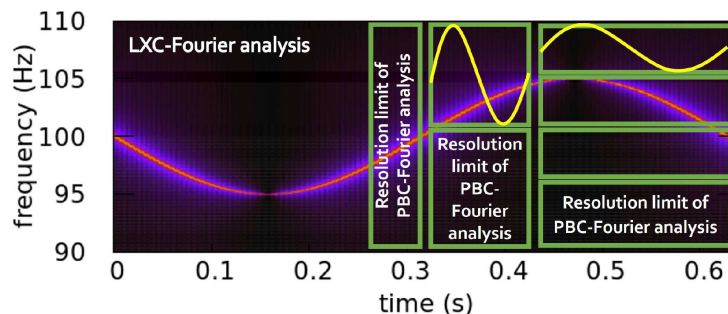


Figure 4: Spectrogram of LXC-Fourier analysis for FM time series [1]. Frequency-width \times time-width is always 1 Hz \cdot s for PBC-Fourier analysis.

Its central frequency is 100 Hz, frequency deviation is ± 5 Hz, and sampling frequency is 10 kHz [1]. Inserted pixels show the time-frequency resolution limit of conventional PBC-Fourier analysis. Detail of the frequency deviation is not visible with the PBC-Fourier analysis, because of its resolution limit.

3 Analysis of lung sounds with abnormalities

We use a data set of lung sounds [4] with 4 kHz sampling, which is recorded using a digital stethoscope with active noise cancellation, and with built-in frequency filters 100 – 500 Hz.

Various lung sounds are recorded. Among them, we chose the lung sounds with abnormalities named “crackles” with random pulse series, and “wheezing” with constant frequency. In addition, we chose a normal lung sound for reference.

We apply the LXC-Fourier analysis with the parameters of $M = 6$, and $N = 20$, and plot the obtained central frequencies $f_m(t)$ above 50 Hz in Fig. 5(L),

and their corresponding instantaneous spectra Eq. (14) in Fig. 5(R). A frequency filter $f_m(t) > 50$ Hz is applied to remove the low frequency background terms below the frequency range of the digital stethoscope, such an example is the constant term (no. 1) in Fig. 3(b). This kind of filtering (removing unnecessary information) is valuable to focus on the information which we want. Note that the computation error term (no. 4) in the figure is also the term unnecessary.

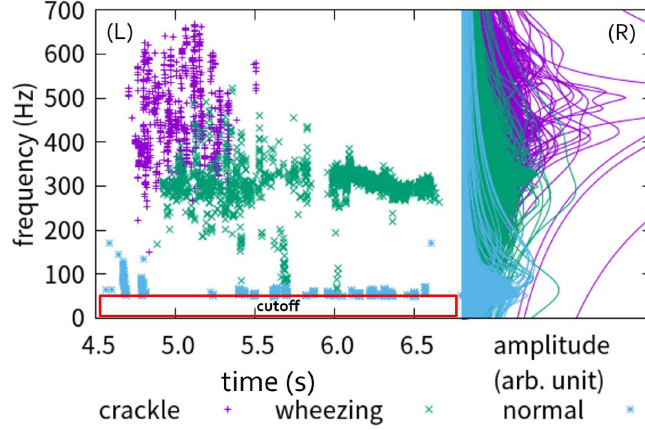


Figure 5: Obtained results for three lung sounds (crackles, wheezing, normal). (L) Central frequencies, and (R) corresponding instantaneous spectra.

The central frequencies of crackles scatter between 300 and 700 Hz, and their corresponding instantaneous spectra also scatter around the region. As the time series of crackles is a pulse series, each pulse decays rapidly, each $|\lambda_m(t)|$ becomes large, and each instantaneous spectrum becomes broad.

Note that the central frequencies appear above the frequency range of the digital stethoscope (up to 500 Hz). It is the reflection of high intensities of the pulses, and some consideration for the frequency range will be required.

The central frequencies of wheezing are around 300 Hz, and their corresponding instantaneous spectra gather around the frequency.

The central frequencies of a normal lung sound do not appear in the frequency region above 100 Hz. This means that the obtained central frequencies for crackles and wheezing are from abnormalities.

As we applied a frequency filter to remove low frequency background, the equation for spectrogram becomes

$$F_{>50}(f, t) = \sum_{m=1}^M \sum_{f_m(t) > 50 \text{ Hz}} \left| \frac{c_m(t)\lambda_m(t)}{\lambda_m(t) + 2\pi i(|f_m(t)| - f)} \right|. \quad (17)$$

Various filters are available for the LXC-Fourier analysis. Any combinations of filters are available, such as $|c_m(t)| > c_0$ for enough amplitude, $|\lambda_m(t)| < \lambda_0$ for narrow spectrum, $|\lambda_m(t)/f_m(t)| < A_0$ for relatively narrow spectrum, and $|c_m(t)f_m(t)| > P_0$ for enough power. A filter for enough amplitude was also applied to plot Fig. 5(L).

The spectrograms corresponding to Fig. 5, using Eq. (17), are shown in Fig. 6. Each interested time region is plotted.

The spectrogram of crackles (Fig. 5(a)) shows intermittent structure, because of its impulsive characteristics. Each pulse shows a broad spectrum, and each bright stripe is plotted.

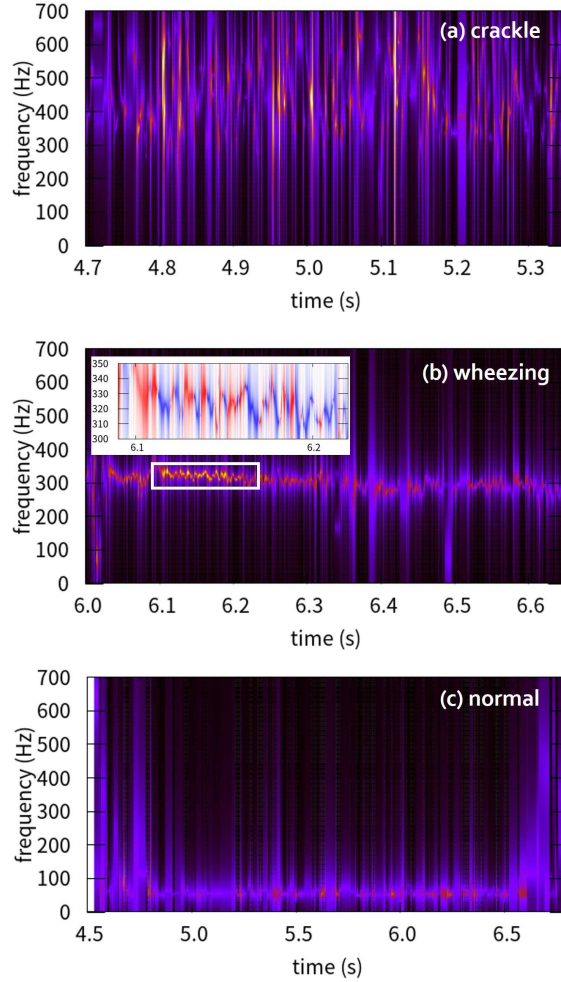


Figure 6: Spectrograms of lung sounds corresponding to Fig. 5. Interested area are plotted. (a) Crackles, (b) wheezing, and (c) normal.

The spectrogram of wheezing (Fig. 5(b)) shows constant frequency around 300 Hz. The insert is the enlargement of the brightest region, which uses Eq. (15) to show additional characteristics. The growing phases (red) and decaying phases (blue) of the lung sound are observed alternately, which structure is a kind of pulse series.

The spectrogram of a normal lung sound (Fig. 5(c)) shows no signal above 100 Hz, and is silent.

Note that the spectrograms with conventional analysis are found in Ref. 4. For example, there are no stripes for crackles.

4 Conclusion

We proposed to replace the PBC-Fourier analysis with the LXC-Fourier analysis. It was shown that the proposed LXC-Fourier analysis theoretically includes the conventional PBC-Fourier analysis, and it overcomes the “theoretical limit of time-frequency resolution” of Fourier analysis.

We introduced the method of instantaneous spectra analysis. Then, we applied the method to the lung sounds with abnormalities (crackles and wheezing) and to a normal lung sound, as a demonstration. Among them, crackles contains a random pulse series.

The spectrum of each pulse is available, and the spectrogram of pulse series is available with assembling each spectrum. As a result, the time-frequency structure of given pulse series is visualized.

As the central frequencies of crackles appear above the frequency range of the digital stethoscope (500 Hz), which means that the frequency range is insufficient, another recording with enough frequency range will be required.

In addition, the time-frequency structure shown in the insert of Fig. 6(b) is another finding. This kind of repetitive grow/decay structure is not visible with the conventional PBC-Fourier analysis, and similar structure will be found in various fields using the LXC-Fourier analysis.

References

- [1] F. Ishiyama, “Refreshing idea on Fourier analysis,” in *Proc. 2025 21st IEEE Colloq. Signal Process. Appl. (CSPA)*, pp. 1-4, 2025.
<https://doi.org/10.1109/CSPA64953.2025.10933386>
<https://doi.org/10.48550/arXiv.2501.03514>
- [2] F. Ishiyama, “Maximum entropy method without false peaks with exact numerical equation,” *J. Phys.: Conf. Ser.*, vol. 1438, 012031 (6pp), 2020.
<https://doi.org/10.1088/1742-6596/1438/1/012031>
- [3] G. Walker, “On periodicity in series of related terms,” *Proc. Roy. Soc. A*, vol. 131, pp. 518-532, 1931.
- [4] Y. Torabi, S. Shirani and J. P. Reilly, “Descriptor: Heart and Lung Sounds Dataset Recorded From a Clinical Manikin Using Digital Stethoscope (HLS-CMDS),” in *IEEE Data Descriptions*, vol. 2, pp. 133-140, 2025.
<https://doi.org/10.1109/IEEEDATA.2025.3566012>
- [5] F. Ishiyama, “Nonlinear trend of COVID-19 infection time series,” *IEICE NOLTA*, vol. 14, pp. 165-174, 2023.
<https://doi.org/10.1587/nolta.14.165>
<https://doi.org/10.48550/arXiv.2404.00866>
- [6] F. Ishiyama and R. Takahashi, “The bounce hardness index of gravitational waves,” *Class. Quant. Grav.*, vol. 27, 245021 (11pp), 2010.
<https://doi.org/10.1088/0264-9381/27/24/245021>
<https://doi.org/10.48550/arXiv.1009.0608>
- [7] B. van der Pol, “The fundamental principles of frequency modulation,” *J. Inst. Elect. Eng. III*, vol. 93, pp. 153-158, 1946.

- [8] R. Kubo, “Statistical-mechanical theory of irreversible process. I. General theory and simple applications to magnetic and conduction problems,” *J. Phys. Soc. Jpn.*, vol. 12, pp. 570-586, 1957.
<https://doi.org/10.1143/JPSJ.12.570>
- [9] I. Daubechies, J. Lu, and H. T. Wu, “Synchrosqueezed wavelet transforms: An empirical mode decomposition-like tool,” *Appl. Comput. Harmon. Anal.*, vol. 30, pp. 243-261, 2011.
- [10] F. Ishiyama, “Providing unique solution to Daubechies’s AM-FM oscillator expansion, and its limitations,” in *Proc. 2023 19th IEEE Colloq. Signal Process. Appl. (CSPA)*, pp. 13-18, 2023.
<https://doi.org/10.1109/CSPA57446.2023.10087433>
- [11] F. Ishiyama, “Theoretical and computational study of nonlinear series expansion for nonlinear system identification,” in *Proc. 2025 21st IEEE Colloq. Signal Process. Appl. (CSPA)*, pp. 5-8, 2025.
<https://doi.org/10.1109/CSPA64953.2025.10933287>
- [12] <https://github.com/fishiyama/thesis-suppl/>
- [13] F. Itakura, “Minimum prediction residual principle applied to speech recognition,” *IEEE Trans. Acoust. Speech Signal Process.*, vol. 23, pp. 67-72, 1975.

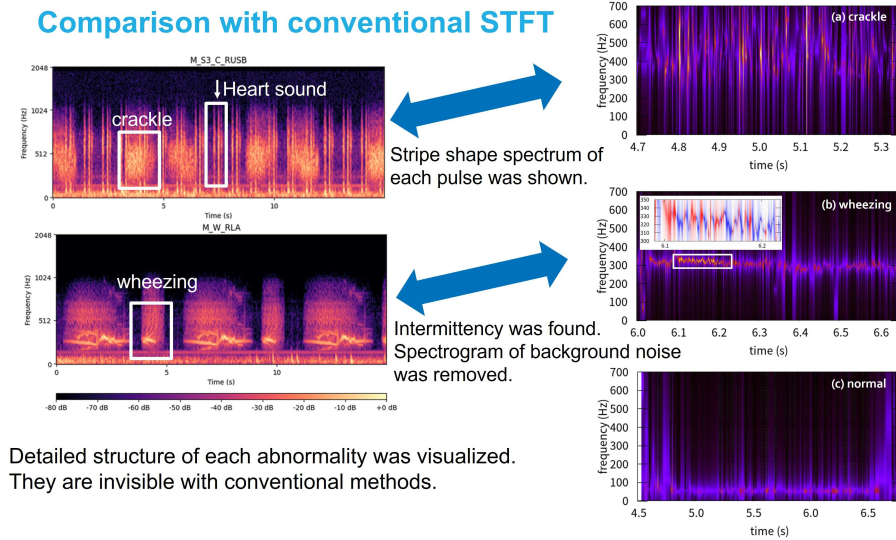


Figure 7: Comparison with conventional method [4].